The impact of cable spacing on the behavior of cable-stayed bridges

R. Al-Rousan*
Jordan University of Science and Technology, Irbid, Jordan
* E–mail: rzalrousan@just.edu.jo

Keywords: engineering, cable-stayed bridge, technology, civil engineering, structural concrete deck

Abstract. This paper aims to find the optimum cable spacing in terms of vertical deformation and cable stress for static and dynamic analysis. To achieve the objective of this study six models are developed using ABAQUS with six different cable spacing ((8.04 m, 30 cables), (9.42, 25), (11.11, 22), (13.72, 18), (15.56, 16), and (16.67, 15)). Firstly, a non linear static finite-element analysis is performed on the models; then pretensioning forces are applied to cables, after that the shape modes for each model are presented. Secondly, a nonlinear dynamic analysis is performed on the models; the results obtained from the finite-element analysis are used in the optimization. The results show that the maximum vertical deflection decreased and the cable stress increased with the increasing of cable spacing for both static and dynamic analysis. As a result, the unsupported length increased with the cable spacing increasing; this will lead to larger deflection and greater stresses in the cables. Finally, the optimum cable spacing is 11.2 m based on static and dynamic deflection and cable stress.

1. Introduction

Many types of bridges are used these days. The simplest bridge, the beam bridge, consists of two piers and one beam. However, the need for spans with long distances proposed new alternatives such as suspension bridges and cable-stayed bridges. The cost of the suspension bridges is relatively higher than the cost of the cable-stayed bridges. The elastically supported girder is the main tool in the simulation of the behavior of a cable-stayed girder. The square of the spacing is proportional to the local bending moment between the cables. The newly proposed design necessity that all cables be independently expendable makes closely spaced cables more attractive. It is generally essential that one cable can be dismantled, detensioned, and replaced under reduced traffic loading. The small cable spacing will not increase extremely the additional bending moment in the girder. Accessibility of ever best computer tools helps the engineer to simulate and analysis of the complexity of structure [1–11].

Cable-stayed bridges have been constructed all over the world, are mainly used for medium-to-long spans and are part of important transportation networks. Besides their structural efficiency, they owe their popularity due to an elegant and transparent appearance. The bridges constructed in earthquake-prone areas must be designed to withstand the seismic action. Cable-stayed bridges present long vibration periods, due to the long spans and their flexibility, which theoretically makes them not sensitive to dynamic excitation [10]. However, they feature inherent low damping, and their dynamic behavior is highly dependent on the stiffness and mass distribution. Therefore, any attempt to minimize the inertia forces and to maximize the resistance leads to an undesired decrease in the vibration periods and consequently to higher seismic forces. Furthermore, although concrete bridges feature higher damping than steel or composite bridges, they are also heavier, which implies higher inertia forces.

The dynamic behavior of cable-stayed bridges has been extensively studied by several authors. Abdel-Ghaffar and Nazmy [12] considered a three-dimensional model, including the geometrical nonlinearities, to

study the dynamic behavior of long-span cable-stayed bridges under seismic loading. The cases of synchronous and non-synchronous support excitations were considered, and the effects of the non-dispersive traveling seismic wave on the bridge response were studied. Abdel-Ghaffar and Khaliffa [13] studied the dynamic behavior of cable-stayed bridges focusing on the importance of the cables' vibrations in the overall dynamic response of these bridges. Soneji and Jangid [14] studied the influence of dynamic soil-structure interaction on the behavior of seismically isolated cable-stayed bridges. Caetano et al. [15] focused on modeling the dynamic behavior of cable-stayed bridges. The authors developed a three-dimensional finite element model that includes the cable transversal motion and were tuned based on repeated campaigns of vibration data acquisitions of a cable-stayed bridge. Camara and Efthymiou [16] studied the deck-tower interaction in the transverse seismic response of cable-stayed bridges. The authors considered the contribution of different vibration modes and the influence of the main span length, the tower shape, the cable-system arrangement, the width and height of the deck, and the soil conditions. Concerning the optimization of cable-stayed bridges under seismic action only a few studies have been reported. Negrão and Simões [17] optimized steel cable-stayed bridges under seismic action considering both modal/spectral and time-history approaches. The cable areas and the cross-sectional dimensions of the deck and towers were considered as design variables. Fereira and Simões [18] presented an algorithm for the optimum design of steel cable-stayed bridges considering active devices to control the response of the structure subjected to earthquakes.

Cable-stayed bridge design involves some complex problems, such as: defining the structural system, finding the members' cross-sections, the calculation of the cable forces distribution, the construction stages, and geometrical nonlinear effects. For concrete bridges, the time-dependent effects must also be considered. The seismic action adds more complexity to find an adequate mass and stiffness distribution that optimizes the dynamic bridge response. Therefore, optimization algorithms are particularly used to handle a large amount of information involved and thus, obtaining economical and structurally efficient solutions under both static and dynamic loading. Previous works concerning the optimization of cable-stayed bridges studied the cable forces calculation in steel [19, 20], composite [21, 22] and concrete bridges [23, 24]. The use of geometric and cross-sectional design variables was also reported in the optimization of steel and composite steel-concrete bridges [25] subjected to static loading. The main objective was to minimize the structural cost while ensuring that the stresses and displacements throughout the structure remain within allowable limits.

We are faced with a large optimization problem given the number of design variables and objectives representing several load cases, the consideration of geometrical nonlinearities and the dynamic analysis to access the structural response under seismic action. A cable-stayed bridge needs, including the time-dependent effects and poses additional difficulties to the optimization problem when formulating the sensitivities of the design objectives. This is due to the fact that the resistance of each cable-stayed bridge depends on the correspondent cross-sectional design variables.

2. Methods

The goal of this analysis is to determine the spacing of the optimum cable; the different models will be studied using ABAQUS. Eighteen models will be created and analyzed which have the same parameters except the cable spacing and the deck stiffness (three-deck stiffness and six cables spacing). The eighteen models are created based on design constants will be described later in this chapter, computer analyses will be conducted, then the optimum cable spacing and optimum deck stiffness will be calculated based on the results.

2.1. Design constants

A doubly symmetrical cable-stayed bridge about the two major axes with one middle span (500 meters long) and two side spans (250 meters each span) will be used; the bridge will have four towers (two at each side of the deck) as shown in Figure 1. The typical ratio which offers an economical solution for the design for the height to the main span ratio is 5, according to this ratio, the height of the towers is 100 m. The typical design range for the pylons to the towers' ratio is 2, so the height of piers is 50 m. The cross-section of the towers is (3.5 m × 5.5 m) of conventional concrete C30; this cross-section needs about 1.2 m^2 longitudinal reinforcement. The cable's material is a seven-wired strand T15S 1770 which has a diameter of 20 cm, modulus of elasticity equal to 165 GPa and the Poisson's ratio of 0.3. Based on the history of the cable-stayed bridges, the most preferred layout of the cable's arrangement is the double-plane semi-fan system, which provides better support to the deck. A reinforced concrete (RC) deck is used, the deck consists of 0.25 m thick. The steel used for the girders has an elastic modulus of 200 GPa, and Poisson's ratio of 0.3 and the mechanical prosperities of the RC slab are $f'c$ of 50 MPa, Poisson's ratio of 0.15 and normal weight density of 2400 kg/m^3. The deck has four traffic lanes, two lanes at each side and a pedestrian walkway at each side too, the width of the deck will be taken is 25 m. For the boundary, the towers are fixed at their ends, and the deck is pinned at its ends, the intersection between the towers and the deck are pinned too.
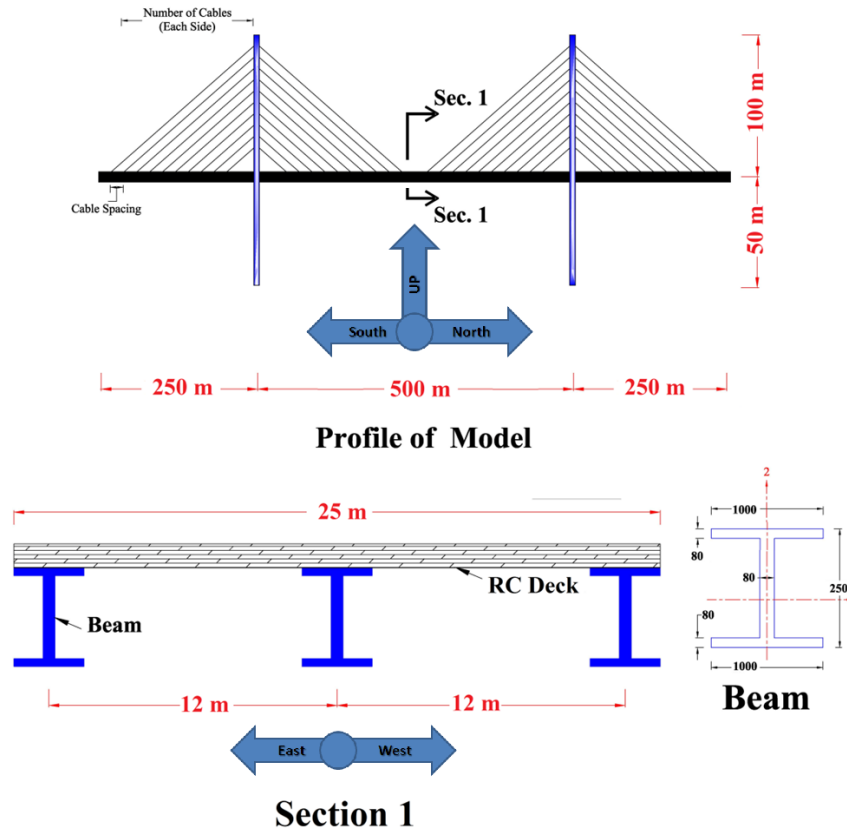
Figure 1. Bridge details and loading directions.

2.2. Finite elements

Thick shell element is suitable for the analysis of RC and sandwich shells (RC decks). Irregular meshes of S8R elements converge very poorly because of severe transverse shear locking; therefore, this element is recommended for use in usual mesh geometries for thick shell applications. As a conclusion, a S8R thick shell element with typical mesh geometries will be used for meshing the RC deck. The 3-node quadratic beam element (B32) will be used for meshing the Girders, the Cross-Beams, and the towers. Finally, the 2-node linear interpolation truss element (T3D2) will be used for meshing the cables. Truss elements (T3D2) are one-dimensional bars or rods that are assumed to deform by axial stretching. These elements pin jointed at their nodes, and so only translationally displacements and the initial position vector at each node are used in the discrimination. When the strains are large, the formulation is simplified by assuming that the trusses are made of incompressible material. There are two truss elements in Bequest: a 2-node linear interpolation truss and a 3-node quadratic interpolation truss. The quadratic interpolation version is in the library, mainly for compatibility with the quadratic interpolation elements of other types, such as a shell element S8R5. The same interpolation functions are used for both the Cartesian displacement components and for the Cartesian components of the initial position vector, so these elements are the simplest form of nonparametric elements.

2.3. Models

Table 1 shows the simulated models to be analyzed; every model has different spacing for the cables as results of six different models. It is common knowledge that the cables work more effectively when they form angles between (25–65°) with the deck, and it is very common for cable-stayed bridges to have been spacing between 8.04 m to 16.67 m between cables. The deck supported on three I-steel beams, as shown in Figure 1. All models arrangement leads to minimum and maximum angles of 22.7° and 66.12° respectively. The cable spacing and the number of cables in each side for the first, second, third, fourth, fifth, and sixth model will be taken (8.04 m, 30 cables), (9.42, 25), (11.11, 22), (13.72, 18), (15.56, 16), and (16.67, 15), respectively. The total number of cables for the model equals eight times the number of cables on each side. Shell elements were used to represent the RC slab; tie connections were used to connect the slab with the steel frame; the steel frame consists of the steel girders and cross beams. The cross beams have the same dimensions as the steel girders for simplification. Beam elements were used to represent the steel frame. The cables and girders are connected using MPC constraint's pin type, and the towers and cables are connected using MPC constraint's tie type. The cables are represented using truss elements, and beam elements were used for representing the towers.

Table 1. Details of simulated models and static results.

Model Number	Cable Spacing (m)	Number of cables (Each Side)	$\Delta_{Max,B}$, m	$\Delta_{Max,A}$, m	$\sigma_{Max,B}$, MPa	$\sigma_{Max,B}/\sigma_u$, %	$\sigma_{Max,A}$, MPa	$\sigma_{Max,A}/\sigma_u$, %
B1CS8.04	8.04	30	6.16	0.05029	641	40	173	9.8
B1CS9.42	9.42	25	9.68	0.06195	723	64	191	10.8
B1CS11.11	11.11	22	9.34	0.06155	829	62	190	10.7
B1CS13.72	13.72	18	10.71	0.06135	1001	76	264	14.9
B1CS15.56	15.56	16	7.08	0.0488	1365	52	457	25.8
B1CS16.67	16.67	15	8.61	0.04419	1049	65	248	14.0

Note: $\Delta_{Max, B}$: Maximum deflection before pre-tensioning; $\Delta_{Max, A}$: Maximum deflection after pre-tensioning; $\sigma_{Max, B}$: Maximum stress in cables before pre-tensioning; $\sigma_{Max,A}$: Maximum stress in cables after pre-tensioning; σ_u: Ultimate stress of cable.

2.3.1. Static Loading

In accordance to AASHTO, the load combination has been taken into account for the static case is "STRENGTH I", which is equal to:

$$T.L = 1.25 \times D.L + 1.5 \times S.D.L + 1.75 \times L.L, \tag{1}$$

where $T.L$ is the factored total load;

$D.L$ is the dead load;

$S.D.L$ is the superimposed dead load,

$L.L$ is the live load. The static load applied as pressure on the deck surface in the gravity direction. Nonlinear analysis was performed to account for the nonlinear performance of the cables.

2.3.2. Pre-tensioning

The conventional «Zero-Displacement» method proposed by Wang et al. [21] was used to achieve the pre-tensioning forces in the cables. Firstly, the towers were restricted from the vertical and horizontal movements, and then prestressing forces were applied to the cables until a zero vertical displacement at the center of the mid-span is achieved. After that, the towers were allowed to move in the vertical and horizontal directions. Finally, the prestressing forces were adjusted until we had zero vertical displacements at the span center.

2.3.3. Earthquake Loading

The earthquake – time history that has been used is the AQABA earthquake, as shown in Figure 2. AQABA earthquake happened on 22/11/1995 and the station that record the time history is "Eilat" station; the earthquake had peak ground acceleration (PGA) = 0.109g (Figure 2) in the vertical direction (UP) (Figure 1), 0.086g (Figure 2) in the horizontal direction (North-South) (Figure 1) and 0.097g (Figure 2) in the horizontal direction (East-West) (Figure 1) and its lasted for sixty seconds. In accordance to AASHTO, the "EXTREME EVENT I" load combination has been taken into account for the dynamic case:

$$T.L = 1.25 \times D.L + 1.5 \times S.D.L + 0.5 \times L.L + 1.0 \times EQ, \tag{2}$$

where EQ is the earthquake loading. The earthquake loading was applied at the ends of the towers and the dead load, superimposed dead load, and the live load was applied as pressure on the surface of the deck.

3. Results and Discussion

3.1. Static analysis

Table 1 shows the summary of static analysis results, and Figure 3 shows the deflection due to static loading along the bridge before and after pre-tensioning. Inspection of Table 1 reveals that the maximum deflections were more than the AASHTO allowable deflection of 0.625 m ($L/800$) in the middle of the mid-span. In addition, the maximum cable stresses were less than the ultimate strength of the cables of 1770 MPa. After applying the pre-tensioning forces in the cables using the Zero-Deflection method, the maximum deflection was reduced to be less than the AASHTO allowable deflection of 0.625 m, as shown in Figure 3. Finally, the maximum stress in cables after pre-tensioning was less than the AASHTO allowable strength of 708 MPa (40 % of the ultimate strength of the cable).
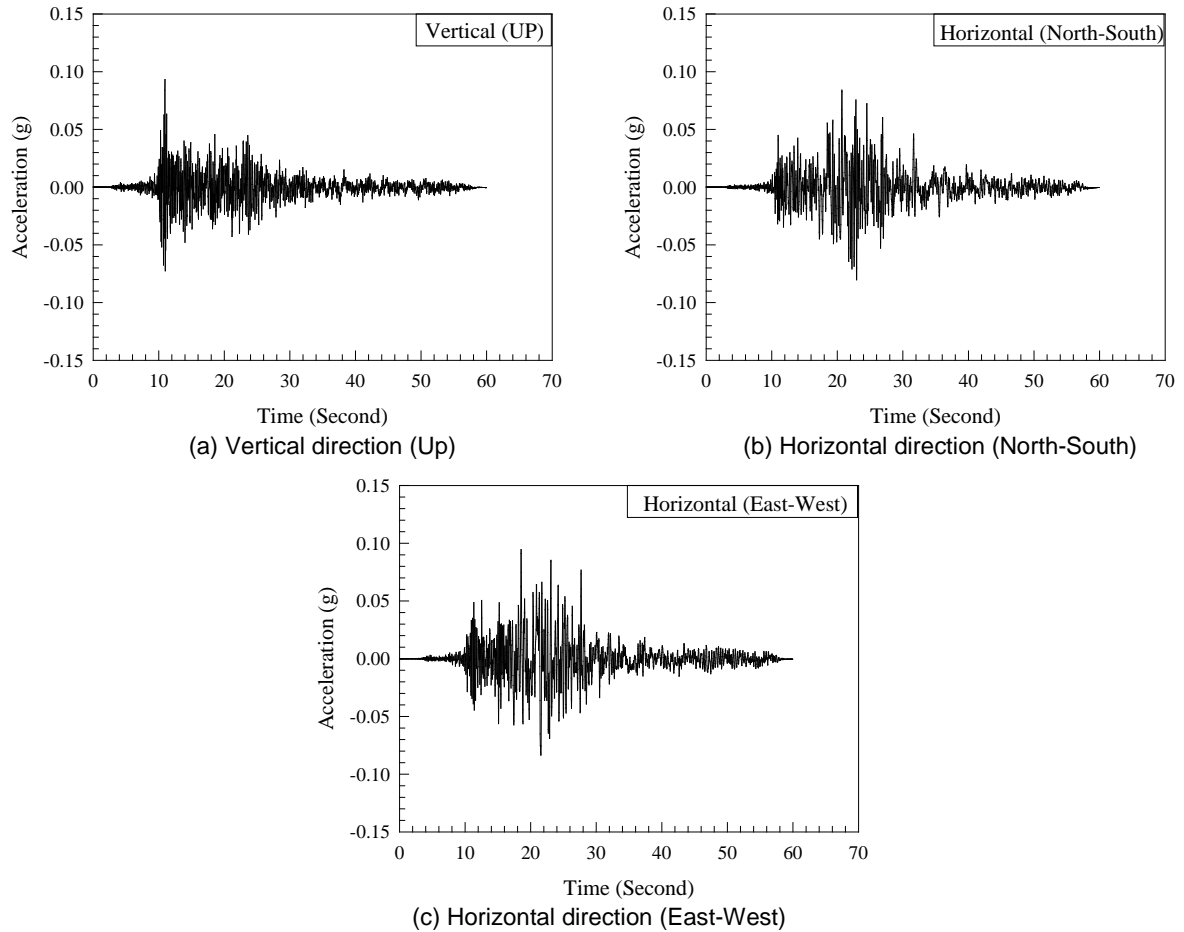
Al-Rousan Rajai

(a) Vertical direction (Up)

(b) Horizontal direction (North-South)

(c) Horizontal direction (East-West)

Figure 2. AQABA earthquake acceleration – time history.

3.2. Modes of the bridge with the corresponding natural frequencies

Figure 4 shows the typical ten modes of the bridge with the corresponding natural frequencies for the bridge. Mode one represents the symmetrical lateral movement of the towers; mode two represents an anti-symmetrical lateral movement of the towers; mode three represents the cross movement of the towers; mode four represents symmetrical lateral movement of the towers – adjacent towers move in opposite direction; mode five represents the symmetrical torsion of the deck; mode six represents the symmetrical bending of the deck, mode seven represents the anti-symmetrical bending of the deck; mode eight represents the symmetrical torsion of the deck opposite of Mode five, mode nine represents the anti-symmetrical torsion of the deck, and finally mode ten represents the lateral planer bending of the deck. Inspection of Figure 4 reflected that all-natural frequencies are below 0.70 cycles/s. Moreover, mode ten had the highest natural frequency of 0.69564 cycles/s; while mode one had the lowest natural frequency of 1.1124 cycles/s. Finally, mode eight, which is the opposite of mode five, had a natural frequency of 1.55 times the natural frequency of mode five. Therefore, the sequence of natural frequency for the ten modes is classified as following from the strongest to the weakness: the lateral planer bending, the symmetrical bending, symmetrical torsion, and symmetrical lateral movement.

Table 2. Summary of dynamic analysis results.

Model Number	$\Delta_{Max,S}$, m	$\sigma_{Max,S}$, MPa	$\sigma_{Max,S}/\sigma_u$, %	$\Delta_{Max,D}$, m	$\sigma_{Max,D}$, MPa	$\sigma_{Max,D}/\sigma_u$, %	$\dfrac{\Delta_{Max,D}}{\Delta_{Max,S}}$, %	$\dfrac{\sigma_{Max,D}}{\sigma_{Max,S}}$, %
B1CS8.04	0.05029	173	9.8	0.1437	214	12.1	35.0	123.7
B1CS9.42	0.06195	191	10.8	0.2187	250	14.1	28.3	130.9
B1CS11.11	0.06155	190	10.7	0.1727	246	13.9	35.6	129.5
B1CS13.72	0.06135	264	14.9	0.2091	341	19.3	29.3	129.2
B1CS15.56	0.0488	457	25.8	0.1935	357	20.2	25.2	78.1
B1CS16.67	0.04419	248	14.0	0.2151	383	21.6	20.5	154.4

Note: $\Delta_{Max,S}$: Maximum deflection due to static loading; $\Delta_{Max,D}$: deflection due to dynamic loading; $\sigma_{Max,S}$: Maximum stress in cables due to static loading; $\sigma_{Max,A}$: Maximum stress in cables due to dynamic loading; σ_u: Ultimate stress of cable.
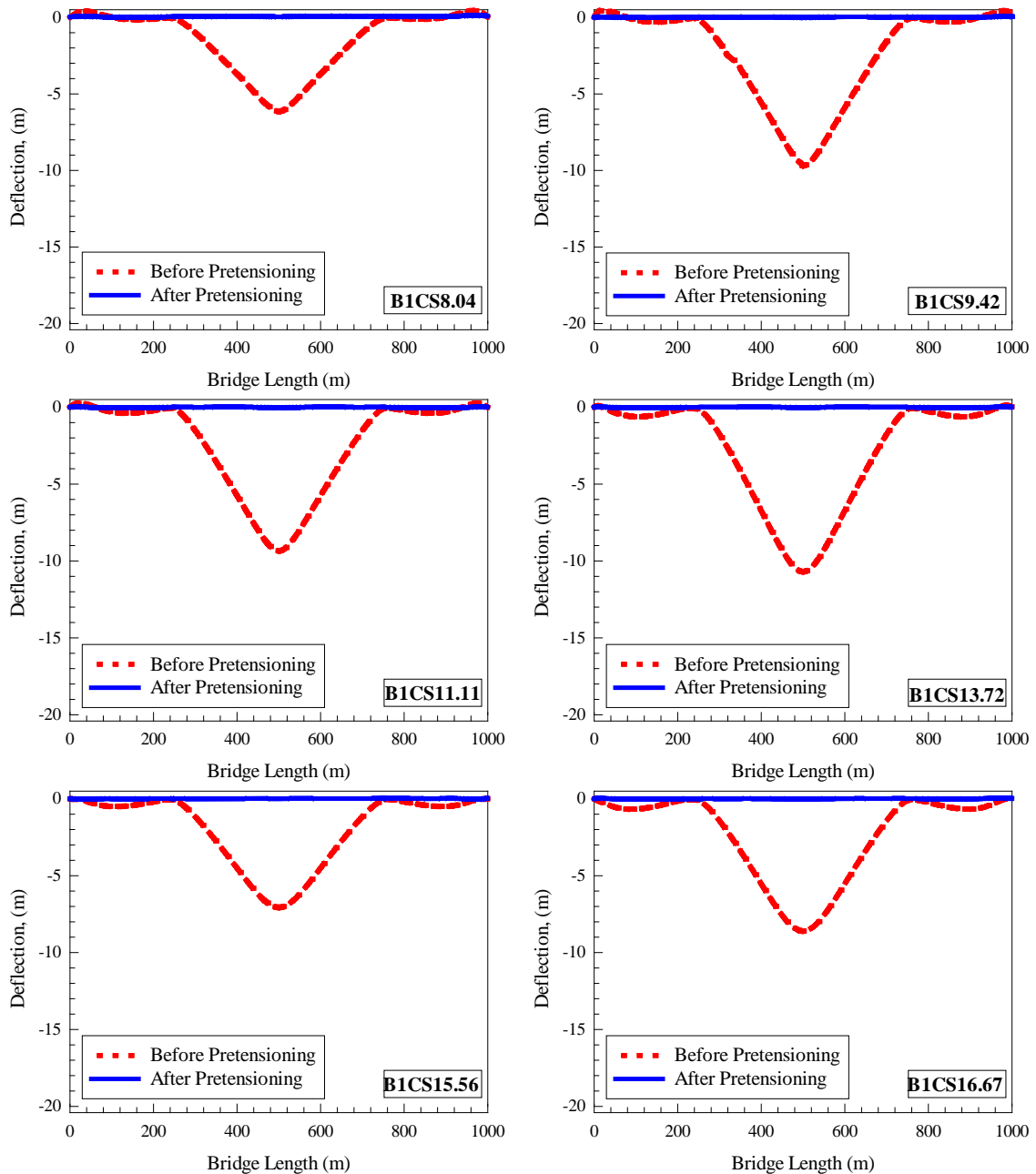
Figure 3. Typical deflection along the bridge before and after pre-tensioning.

3.3. Dynamic analysis

AQABA 1995 earthquake was applied on the bridge in three directions (UP, North-South, and East-West) as shown in Figure 2. Each direction had an acceleration-time history; the earthquake was applied to the supports. Table 2 shows the summary of dynamic analysis results, and Figure 5 shows the deflection along the bridge due to static and dynamic loading. Inspection of Figure 5 and Table 2 reveal that the maximum deflections due to static and dynamic loading were less than the AASHTO allowable deflection of 0.625 m. Also, the maximum cable stresses behave the same as maximum deflection, which is less than the AASHTO allowable strength of 708 MPa. In addition, Table 2 shows that the deflection and stress in the cable due to dynamic loading is more than static ranged from 20-35% and 78-154%, respectively. Therefore, the effect of dynamic loading had a higher impact on the maximum vertical deflection than maximum stress in the cables.

3.4. Optimum cable spacing

Figure 6 shows the maximum deflection due to static loading ($\Delta_{Max,S}$), maximum deflection due to dynamic loading ($\Delta_{Max,D}$); maximum stress in cables due to static loading ($\sigma_{Max,S}$); maximum stress in cables due to dynamic loading ($\sigma_{Max,A}$) were normalized with respect to value of bridge at cable spacing of 8.04 m. The inspection of Figure 6 reveals that the optimum cable spacing is 11.2 m. Figure 6 shows that the vertical deflection increased with the increasing of the cable spacing. Therefore, the maximum vertical deflection decreased, and the cable stress increased as the cable spacing increasing. As a result, the unsupported length increased with the cable spacing increasing; this will lead to larger deflection and greater stresses in the cables.
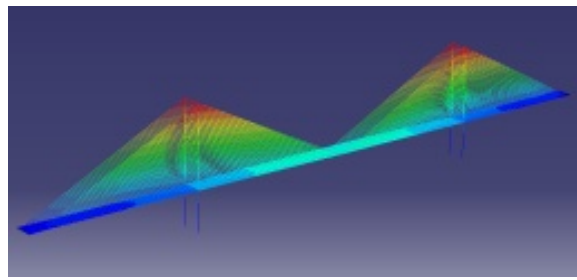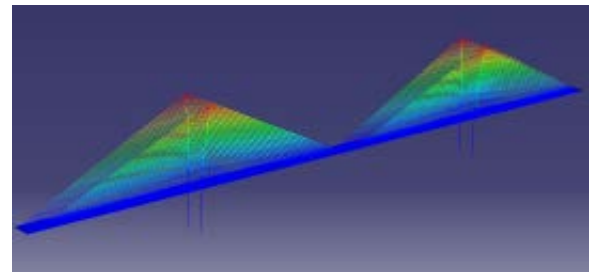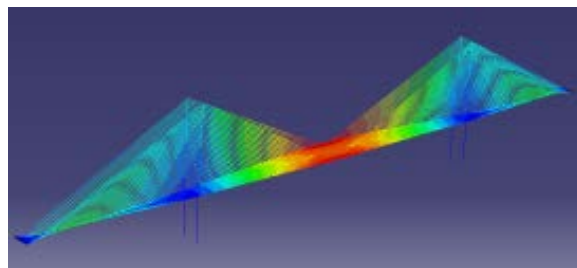
Mode One: Frequency = 1.1124 cycles/s
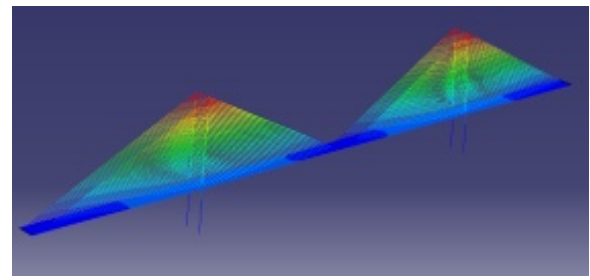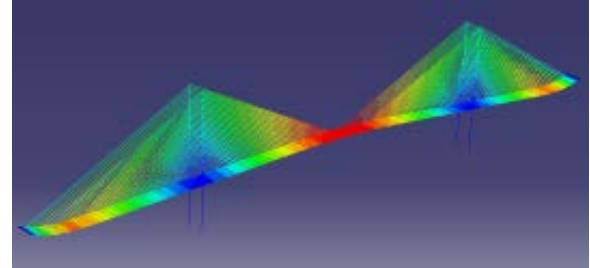
Mode Two: Frequency = 0.12012 cycles/s
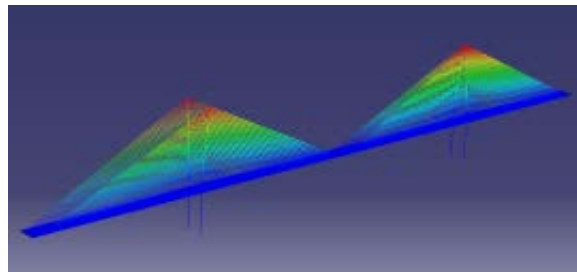
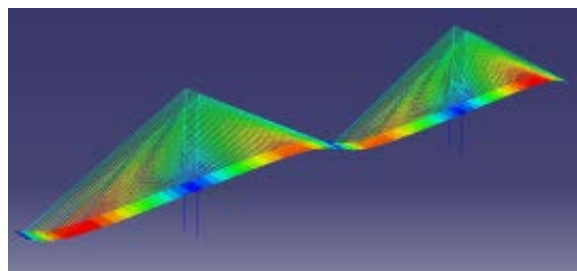Mode Three: Frequency = 0.1677 cycles/s
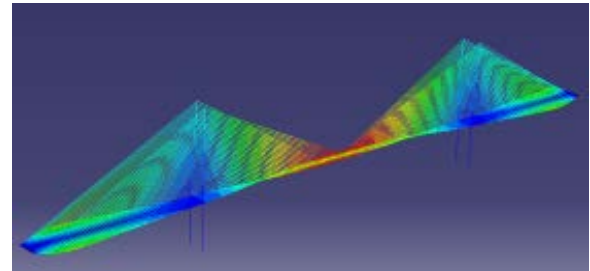
Mode Four: Frequency = 0.20124 cycles/s

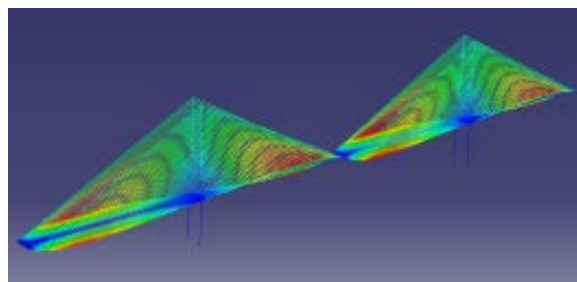Mode Five: Frequency = 0.32775 cycles/s
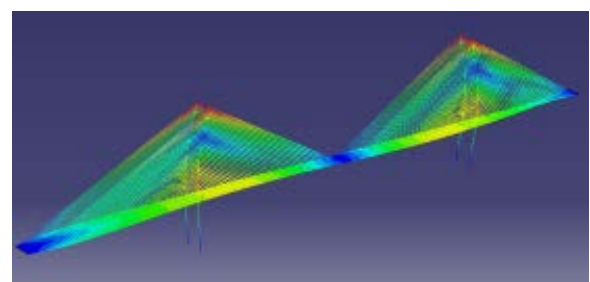
Mode Six: Frequency = 0.36096cycles/s

Mode Seven: Frequency = 0.46584 cycles/s

Mode Eight: Frequency = 0.49956cycles/s

Mode Nine: Frequency = 0.56496 cycles/s

Mode Ten: Frequency = 0.69564 cycles/s

Figure 4. Typical mode shape obtained from B1CS8.04.

3.5. Optimization

The relation between cable spacing and deformation of the bridge will be formed for each deck, and then the optimum cable spacing will be found from these equations. Secondly, the optimum deck stiffness for each cable spacing was found. The approximate equation that can be used to represent the deformation and the cable spacing is:

$$u_i(x) = \alpha_0 + \alpha_1 x_i + \alpha_2 x_i^2 + \alpha_3 x_i^3 + \alpha_4 x_i^4 + \alpha_5 x_i^5; \quad i = 1, 2, 3, 4, 5, 6; \tag{3}$$
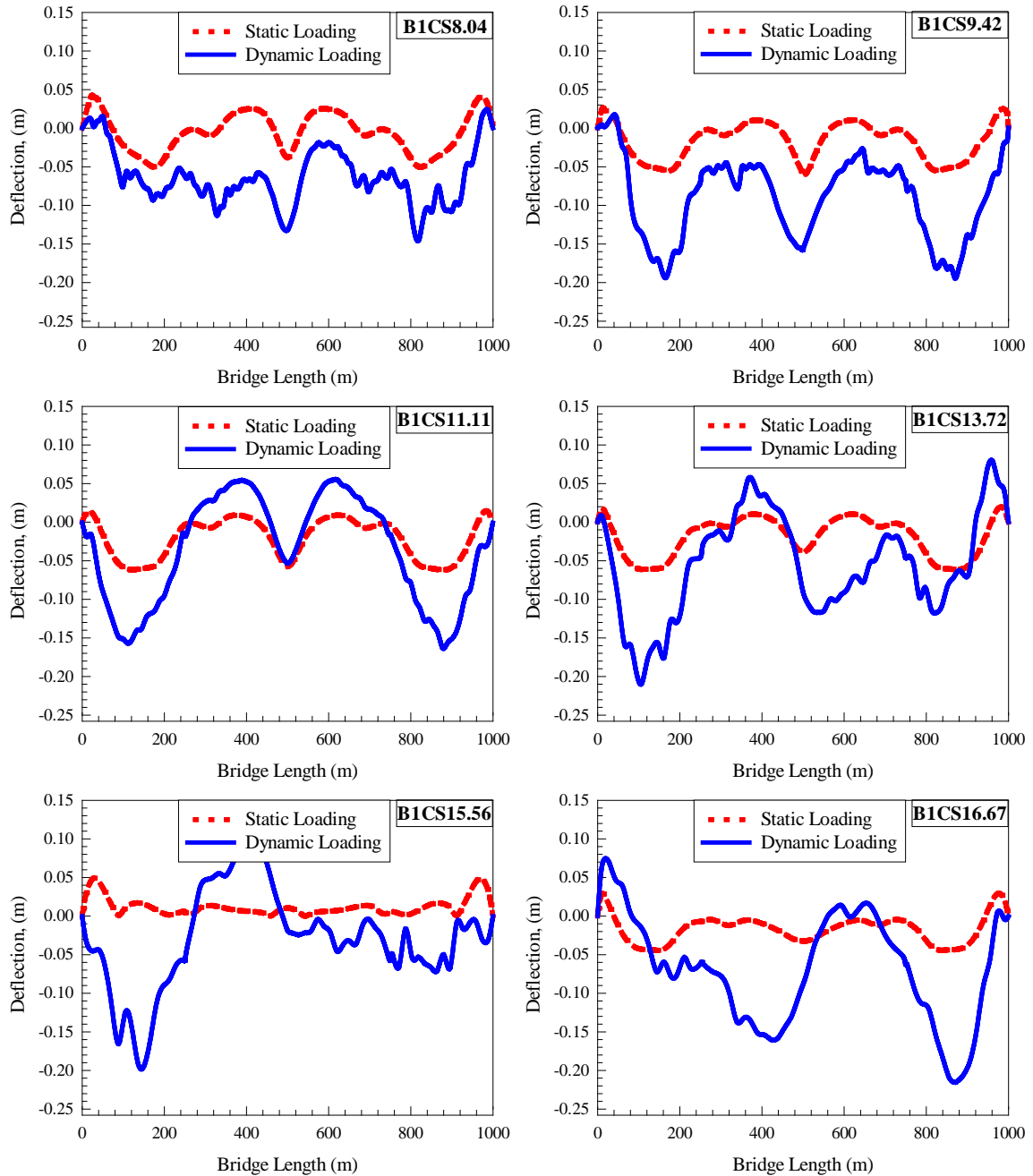
Al-Rousan, Rajai

Figure 5. Typical deflection along the bridge due to static and dynamic loading.

$$
\begin{Bmatrix} u_1(x) \\ u_2(x) \\ u_3(x) \\ u_4(x) \\ u_5(x) \\ u_6(x) \end{Bmatrix} = \begin{Bmatrix} 1 & x_1 & x_1^2 & x_1^3 & x_1^4 & x_1^5 \\ 1 & x_2 & x_2^2 & x_2^3 & x_2^4 & x_2^5 \\ 1 & x_3 & x_3^2 & x_3^3 & x_3^4 & x_3^5 \\ 1 & x_4 & x_4^2 & x_4^3 & x_4^4 & x_4^5 \\ 1 & x_5 & x_5^2 & x_5^3 & x_5^4 & x_5^5 \\ 1 & x_6 & x_6^2 & x_6^3 & x_6^4 & x_6^5 \end{Bmatrix} \times \begin{Bmatrix} \alpha_0 \\ \alpha_1 \\ \alpha_2 \\ \alpha_3 \\ \alpha_4 \\ \alpha_5 \end{Bmatrix}; \tag{4}
$$

$$
\{\alpha\} = [x]^{-1}\{u\}, \tag{5}
$$

where $u(x)$ is the maximum deformation in meters and x is the cable spacing in meters. The constants α_0, α_1, α_2, α_3, and α_4 can be solved using the values of Table 2. Using MATLAB for solving the previous matrices, the constants were calculated and the derived function becomes:

Al-Rousan Rajai

$$u(x) = 0.0002x^5 - 0.0136x^4 + 0.3386x^3 - 4.1599x^2 + 25.148x - 59.607. \tag{6}$$
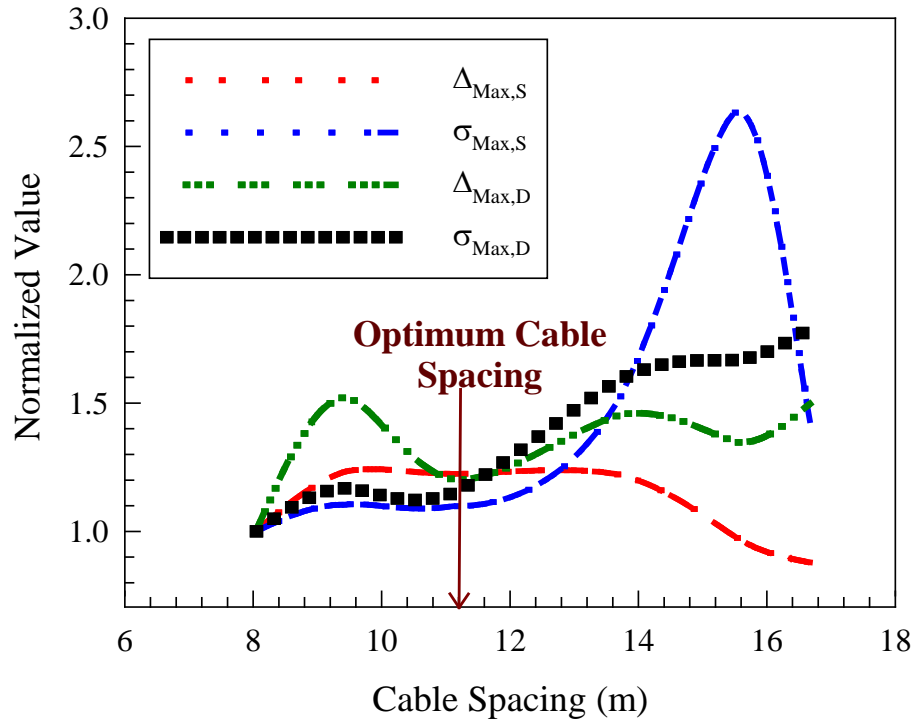

Figure 6. The normalized value of studied parameters with cable spacing ($\Delta_{Max,S}$: Maximum deflection due to static loading; $\Delta_{Max,D}$: deflection due to dynamic loading; $\Delta_{Max,S}$: Maximum stress in cables due to static loading; $\Delta_{Max,A}$: Maximum stress in cables due to dynamic loading).

Equation (6) is plotted in Figure 7, which reflected that a cable spacing greater than 15 m is not possible and less than 8.5 m is too dense. After differentiation once, at cable spacing of 11.2 m, the function has a local minimum, u = 0.11 m. In terms of bridge design, 22 cables with cable spacing of 11.11 m are needed on each side of each tower, by using Equation (6) the deformation equal to 0.1717 m.
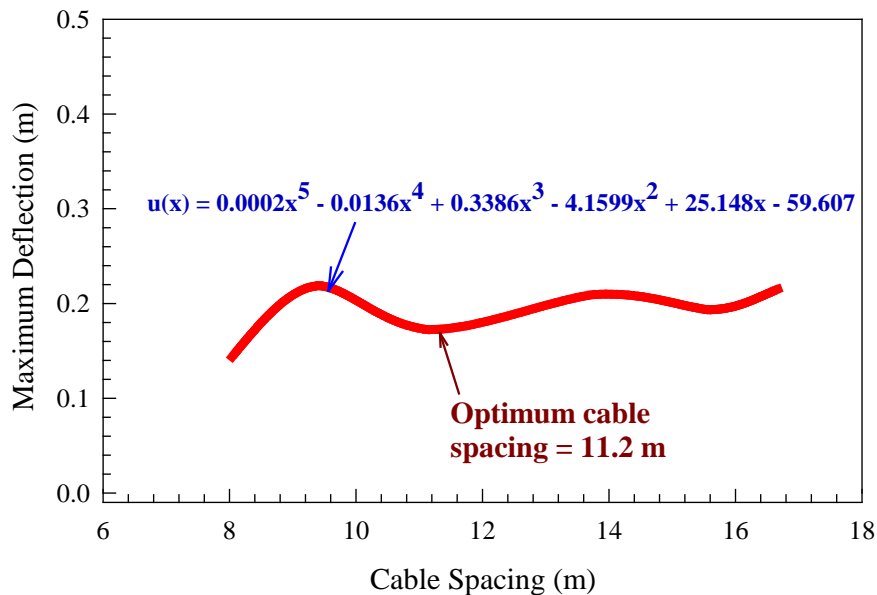

Figure 7. Maximum deformation with cable spacing.

3.6. Materials consumption and total cost

Al-Rousan et al. [10] show that the initial cost of the FRP decks is significantly higher than the reinforced concrete decks; however, the life cycle cost of FRP decks is comparable to the cost of RC decks. Al-Rousan et al. [10] also indicated that the use of the FRP deck instead of the concrete deck would lead to fewer deformations and fewer stresses in the bridge because of the lightweight of the FRP material and the cost of FRP deck is acceptable than the concrete deck for long term stage. Also, the initial cost of the steel bridge

deck is significantly higher than the reinforced concrete bridge deck. However, the use of concrete in the bridge deck is probable to decrease the maintenance cost and increase the service life because the concrete does not exhibit corrosion problems than steel materials.

4. Conclusions

This paper aims to find the optimum cable spacing in terms of vertical deformation and cable stress for static and dynamic analysis. To achieve the objective of this study six models are developed using ABAQUS with six different cable spacing ((8.04 m, 30 cables), (9.42, 25), (11.11, 22), (13.72, 18), (15.56, 16), and (16.67, 15)). The following conclusions are drawn based on the findings of this study:

1. For static loading, the maximum vertical deflection decreased, and the cable stress increased with the increasing of cable spacing.

2. The dynamic loading had more inverse effect on the vertical deflection and direct effect on the cable stress than static loading

3. The cable stresses and the maximum deck deflection increased as the spacing between cables increased. As a result, the unsupported length increased with the cable spacing increasing; this will lead to more significant deflection and higher stresses in the cables.

4. The cable stresses, and the maximum deck deflection increased as the spacing between cables increased. As a result, the unsupported length increased with the cable spacing increasing; this will lead to more significant deflection and more significant stresses in the cables.

5. The cable spacing of 11.2 m is considered as optimum cable spacing in terms of static and dynamic deflection as well as cable stress.

5. Acknowledgments

References

1. Negrão, J., Simões, L. Optimization of cable-stayed bridges with three-dimensional modeling. Computer & Structures. 1997. 64(1-4). Pp. 741–758. DOI: 10.1016/S0045-7949(96)00166-6
2. Simões, L., Negrão, J. Sizing and geometry optimization of cable-stayed bridges. Computer & Structures. 1994. 52(2). Pp. 309–321. DOI: 10.1016/0045-7949(94)90283-6
3. Simões, L., Negrão, J. Optimization of cable-stayed bridges with box-girder decks. Advances in Engineering Software. 2000. 31. Pp. 417–423. DOI: 10.1016/S0965-9978(00)00003-X
4. Ferreira, L., Simoes, L. Optimum design of controlled cable stayed bridge subject to earthquakes. Structure Multidisc Optimization. 2011. 44. Pp. 517–528. DOI: 10.1007/s00158-011-0628-9
5. Baldomir, A., Hernandez, S., Nieto, F., Jurado, J. Cable optimization of a long span cable stayed bridge in La Coruña (Spain). Advances in Engineering Software. 2010. 41. Pp. 931–938. DOI: 10.2495/OP090101
6. Lute, V., Upadhyay, A., Singh, K. Genetic Algorithms-Based Optimization of Cable Stayed Bridges. Journal Software Engineering and Applications. 2011. 4. Pp. 571–578. DOI: 10.4236/jsea.2011.410066.
7. Wilson, E.L., Kiureghian, A., Bayo, E.P. A replacement for the SRSS method in seismic analysis. Earthquake Engineering and Structural Dynamics. 1981. 9. Pp. 187–192. DOI: 10.1002/eqe.4290090207
8. Ito, M. Cable-supported steel bridges: design problems and solutions. Journal of Construction Steel Research. 1996. 39. Pp. 69–84. DOI: 10.1016/0143-974X(96)00026-0
9. Freire, A.M.S., Negrão, J.H.O., Lopes, A.V. Geometrical nonlinearities on the static analysis of highly flexible steel cable-stayed bridges. Computer Structures. 2006. 84(31-32). Pp. 2128–2140. DOI: 10.1016/j.compstruc.2006.08.047
10. Al-Rousan, R., Haddad, R.H., Al Hijaj, M.A. Optimization of the economic practicability of fiber-reinforced polymer (FRP) cable-stayed bridge decks. Bridge Structures. 2014. 10(4). Pp. 129–143. DOI: 10.3233/BRS-150082
11. Wang, P.H., Tseng, T.C., Yang, C.G. Initial shape of cable-stayed bridges. Journal of Computers Structures. 1993. 46. Pp. 1095–1106. DOI: 10.1016/0045-7949(93)90095-U
12. Abdel-Ghaffar, A.M., Nazmy, A.S. 3-D nonlinear seismic behavior of cable-stayed bridges. J Struct Eng. 1991. 117(11). Pp. 3456–3476. DOI: 10.1061/(ASCE)0733-9445(1991)117:11(3456)
13. Abdel-Ghaffar, A.M., Khalifa, M.A. Importance of cable vibration in dynamics of cable-stayed bridges. J Eng Mech. 1991. 117(11). Pp. 2571–2589. DOI: 10.1061/(ASCE)0733-9399(1991)117:11(2571)
14. Soneji, B.B., Jangid, R.S. Influence of soil–structure interaction on the response of seismically isolated cable-stayed bridge. Soil Dyn Earthq Eng. 2008. 28(4). Pp. 245–257. DOI: 10.1016/j.soildyn.2007.06.005
15. Caetano, E., Cunha, A., Gattulli, V., Lepidi, M. Cable–deck dynamic interactions at the International Guadiana Bridge: on-site measurements and finite element modelling. Struct. Contr. Health Monit. 2008. 15(3). Pp. 237–264. DOI: 10.1002/stc.241
16. Camara, A., Efthymiou, E. Deck–tower interaction in the transverse seismic response of cable-stayed bridges and optimum configurations. Eng Struct. 2016. 124. Pp. 494–506. DOI: 10.1016/j.engstruct.2016.06.017
17. Simões, L.M.C., Negrão, J.H.J.O. Optimization of cable-stayed bridges subjected to earthquakes with non-linear behaviour. Eng Optim. 1999. 31(4). Pp. 457–478. DOI: 0.1080/03052159908941382
18. Ferreira, F.L.S., Simoes, L.M.C. Optimum design of a controlled cable stayed bridge subject to earthquakes. Struct Multidiscip Optim. 2011. 44(4). Pp. 517–528. DOI: 0.1007/s00158-011-0628-9

19. Baldomir, A., Hernandez, S., Nieto, F., Jurado, J.A. Cable optimization of a long span cable stayed bridge in La Coruña (Spain). Adv Eng Softw. 2010. 41(7-8). Pp. 931–938. DOI: 10.2495/OP090101

20. Sung, Y.-C., Chang, D.-W., Teo, E.-H. Optimum post-tensioning cable forces of Mau- Lo Hsi cable-stayed bridge. Eng Struct. 2006. 28(10). Pp. 1407–1417. DOI: 10.1016/j.engstruct.2006.01.009

21. Hassan, M.M. Optimization of stay cables in cable-stayed bridges using finite element, genetic algorithm, and B-spline combined technique. Eng Struct. 2013. 49. Pp. 643–654. DOI: 10.1016/j.engstruct.2012.11.036

22. Hassan, M.M., Nassef, A.O., El Damatty, A.A. Determination of optimum post- tensioning cable forces of cable-stayed bridges. Eng Struct. 2012. 44. Pp. 248–259. DOI: 0.1016/j.engstruct.2012.06.009

23. Martins, A.M.B., Simões, L.M.C., Negrão, J.H.J.O. Optimization of cable forces on concrete cable-stayed bridges including geometrical nonlinearities. Comput Struct. 2015. 155. Pp. 18–27. DOI: 10.1016/j.compstruc.2015.02.032.

24. Martins, A.M.B., Simões, L.M.C., Negrão, J.H.J.O. Cable stretching force optimization of concrete cable-stayed bridges including construction stages and time-dependent effects. Struct Multidiscip Optim. 2015. 51(3). Pp. 757–772. DOI: 10.1007/s00158-014-1153-4

25. Hassan, M.M., Nassef, A.O., El Damatty, A.A. Optimal design of semi-fan cable- stayed bridges. Can J Civ Eng. 2013. 40(3). Pp. 285–97. DOI: 10.1139/cjce-2012-0032

Contacts:

Rajai Al-Rousan, +962799887574; rzalrousan@just.edu.jo